molecular pharmaceutics

articles

Mechanism of Internalization of an ICAM-1-Derived Peptide by Human Leukemic Cell Line HL-60: Influence of Physicochemical Properties on Targeted Drug Delivery

Sumit Majumdar, Naoki Kobayashi, Jeffrey P. Krise, and Teruna J. Siahaan*

Department of Pharmaceutical Chemistry, The University of Kansas, Simons Research Laboratories, 2095 Constant Avenue, Lawrence, Kansas 66047

Received April 23, 2007; Revised Manuscript Received July 5, 2007; Accepted July 9, 2007

Abstract: Peptide-mediated targeted delivery offers an attractive strategy for selective delivery of cytotoxic drugs to cancer cells. In this work, we have investigated the mechanism of internalization of cIBR peptide [cyclo(1,12)PenPRGGSVLVTGC] that is conjugated with fluorescein isothiocyanate (FITC) and doxorubicin (DOX) to give FITC–cIBR and DOX–cIBR conjugates, respectively. Internalization mechanisms of FITC–cIBR and DOX–cIBR were studied in LFA-1-expressing cells (HL-60) and LFA-1-deficient cells (HUVEC) under the following conditions: (a) at two different temperatures (4 and 37 °C), (b) in the presence of ATP-depleting agents (sodium azide and 2-deoxy-D-glucose), and (c) in the presence of a microtubule-disrupting agent (nocodazole). At 37 °C, FITC–cIBR was internalized by HL-60 cells and located in the endosomes; however, it was not internalized by LFA-1-deficient HUVEC. Incubation of FITC–cIBR at 4 °C or in the presence of nocodazole inhibited its endocytosis in HL-60 cells. The ATP inhibitors inhibited the internalization of FITC–cIBR but maintained its binding to cell surface receptors. In contrast, DOX–cIBR was diffusely distributed in the cytoplasm of LFA-1-expressing HL-60 cells following incubation at 37 °C. No inhibitory processes could block the entry or change the distribution pattern of DOX–cIBR into HL-60 cells, suggesting that DOX–cIBR uptake was not mediated by receptors such as LFA-1. DOX–cIBR was still found inside HUVEC, but with a distribution pattern somewhat different from that in HL-60 cells. The major entry mechanism of DOX–cIBR could be via passive diffusion because DOX–cIBR has an octanol/water distribution coefficient (Log D) of 1.15. Thus, DOX–cIBR is more lipophilic than FITC–cIBR with a Log D of 0.57. Therefore, the change in the hydrophobicity of the conjugate may alter the mechanism of entry of DOX–cIBR compared to that of FITC–cIBR. This study suggests that alteration of the physicochemical properties of drug–peptide conjugates can change the mode of uptake from receptor-mediated uptake to passive diffusion.

Keywords: ICAM-1 peptide; LFA-1; endocytosis; doxorubicin; drug conjugate; HL-60 cells; HUVEC

Introduction

Most chemotherapeutic agents are cytotoxic to cells; they eliminate tumor cells on the basis of the rapid growth of these cells compared to normal cells. Unfortunately, it is difficult to avoid drug toxicity against normal cells, which leads to drug side effects. Thus, any method that weakens the side effects of antitumor agents can be of benefit to cancer patients during chemotherapy. One way to weaken drug side effects is to selectively target the drug to tumor cells by utilizing the upregulated and/or activated receptors on the surface of tumor cells. In this case, the ligand for the upregulated receptor is used to selectively direct and carry the drug into tumor cells by covalently conjugating the drug to the ligand.[1–3] For example, the increased level of expression of folate receptors in tumor cells has been

* To whom correspondence should be addressed: Department of Pharmaceutical Chemistry, The University of Kansas, 2095 Constant Ave., Lawrence, KS 66047. Phone: (785) 864-7327. Fax: (785) 864-5736. E-mail: siahaan@ku.edu.

10.1021/mp0700458 CCC: $37.00
Published on Web 08/07/2007

successfully used to target antitumor agents to tumor cells using drug–folate conjugates.[3–5] Due to the higher level of expression of transferrin receptors in tumor cells than in normal cells, transferrin protein and transferrin receptor antibody have been conjugated to cytotoxic molecules (i.e., ricin, doxorubicin) for selectively eliminating tumor cells.[6–10] Other methods for selectively delivering drugs to tumor cells have been investigated, including the use of biodegradable polymers, nanoparticles, peptides, and carbohydrates.

In recent years, cell surface adhesion molecules have been investigated for targeting drugs to tumor cells.[2] Integrins have been shown to undergo endocytosis from the cell surface, and they have been utilized by viruses for infecting the host cells.[11] In cancer cells, there is a selective upregulation of certain integrin receptors. Upregulation of $\alpha_v\beta_3$ and $\alpha_v\beta_5$ integrins on the vascular endothelial cells of solid tumors during angiogenesis has been used to halt angiogenesis or for tumor diagnosis.[2,12] In this case, cyclic RGD peptides that are selective for $\alpha_v\beta_3$ and $\alpha_v\beta_5$ receptors were conjugated to a cytotoxic agent such as doxorubicin (DOX) or paclitaxel for the selective elimination of tumor cells.[12,13] For example, a conjugate between RGD peptide and DOX (DOX–RGD) was shown to improve the survival of mice bearing human breast carcinoma cells (MDA0MB-45).[12] The DOX–RGD conjugate can suppress tumor progression better than DOX alone in this mouse model, suggesting that the conjugate targets the upregulated $\alpha_v\beta_3$ and $\alpha_v\beta_5$ in tumor cells. However, the internalization and localization of RGD peptide conjugates by integrins have not been fully characterized; understanding these processes will provide a better method of selecting a more effective drug to conjugate to the peptide.

In this work, we studied the internalization and localization of an intercellular adhesion molecule-1 (ICAM-1)-derived peptide called cyclic ICAM-1 blocker right [cIBR, cyclo(1,12)-PenPRGGSVLVTGC] that has been shown to bind to isolated $\alpha_L\beta_2$ integrin (LFA-1) and on the surface of T cells.[14,15] Because LFA-1 is expressed only on leukocytes and not on other types of cells (i.e., epithelial and endothelial), this peptide could be used to target drugs to leukocytes for treating leukocyte-related disorders such as leukemia and autoimmune diseases. To follow the mechanism of binding and internalization of cIBR peptide, its N-terminus was conjugated with fluorescein isothiocyanate (FITC) and DOX to give FITC–cIBR and DOX–cIBR conjugates, respectively (Figure 1). The mechanisms of internalization of these conjugates were compared in LFA-1-expressing leukemic cells (i.e., HL-60) and LFA-1-deficient cells (i.e., HUVEC). The hope is that the results from this study can be used to select a better drug–cIBR conjugate for selectively targeting leukocytes.

Experimental Section

Cells and Chemicals. The human acute promyeloid leukemic HL-60 cell line was kindly provided by Y. Zhang (Arizona Cancer Center, University of Arizona, Tucson, AZ). Cells were grown in RPMI 1640 medium supplemented with 10% fetal bovine serum, 100 units/mL penicillin G sodium, 100 μg/mL streptomycin sulfate, and 2.0 g/L $NaHCO_3$. Cells were maintained at a density from 1×10^6 to 2×10^6 cells/mL at 37 °C in a humidified 5% CO_2 atmosphere. HUVEC were purchased from ATCC (Manassas, VA) and grown in DMEM supplemented with 10% fetal bovine serum, 100 units/mL penicillin G sodium, 100 μg/mL streptomycin sulfate, 2.0 g/L $NaHCO_3$, 1.42 g/L HEPES-Na, 1% glutamine, and 1% nonessential amino acids. Doxorubicin hydrochlo-

(1) Garnett, M. C. Targeted Drug Conjugates: Principles and Progress. *Adv. Drug Delivery Rev.* **2001**, *53*, 171–216.
(2) Dunehoo, A. L.; Anderson, M.; Majumdar, S.; Kobayashi, N.; Berkland, C.; Siahaan, T. J. Cell Adhesion Molecules for Targeted Drug Delivery. *J. Pharm. Sci.* **2006**, *95*, 1856–1872.
(3) Lu, Y.; Low, P. S. Folate-Mediated Delivery of Macromolecular Anticancer Therapeutic Agents. *Adv. Drug Delivery Rev.* **2002**, *54*, 675–693.
(4) Lu, Y.; Sega, E.; Leamon, C. P.; Low, P. S. Folate Receptor-Targeted Immunotherapy of Cancer: Mechanism and Therapeutic Potential. *Adv. Drug Delivery Rev.* **2004**, *56*, 1161–1176.
(5) Sudimack, J.; Lee, R. J. Targeted Drug Delivery Via the Folate Receptor. *Adv. Drug Delivery Rev.* **2000**, *41*, 147–162.
(6) Faulk, W. P.; Taylor, C. G.; Yeh, C. J.; McIntyre, J. A. Preliminary Clinical Study of Transferrin-Adriamycin Conjugate for Drug Delivery to Acute Leukemia Patients. *Mol. Biother.* **1990**, *2*, 57–60.
(7) Kovar, M.; Strohalm, J.; Ulbrich, K.; Rihova, B. In Vitro and in Vivo Effect of Hpma Copolymer-Bound Doxorubicin Targeted to Transferrin Receptor of B-Cell Lymphoma 38c13. *J. Drug Targeting* **2002**, *10*, 23–30.
(8) Eavarone, D. A.; Yu, X.; Bellamkonda, R. V. Targeted Drug Delivery to C6 Glioma by Transferrin-Coupled Liposomes. *J. Biomed. Mater. Res.* **2000**, *51*, 10–14.
(9) Kratz, F.; Beyer, U.; Roth, T.; Tarasova, N.; Collery, P.; Lechenault, F.; Cazabat, A.; Schumacher, P.; Unger, C.; Falken, U. Transferrin Conjugates of Doxorubicin: Synthesis, Characterization, Cellular Uptake, and in Vitro Efficacy. *J. Pharm. Sci.* **1998**, *87*, 338–346.
(10) Kratz, F.; Roth, T.; Fichiner, I.; Schumacher, P.; Fiebig, H. H.; Unger, C. In Vitro and in Vivo Efficacy of Acid-Sensitive Transferrin and Albumin Doxorubicin Conjugates in a Human Xenograft Panel and in the Mda-Mb-435 Mamma Carcinoma Model. *J. Drug Targeting* **2000**, *8*, 305–318.
(11) Triantafilou, K.; Takada, Y.; Triantafilou, M. Mechanisms of Integrin-Mediated Virus Attachment and Internalization Process. *Crit. Rev. Immunol.* **2001**, *21*, 311–322.
(12) Arap, W.; Pasqualini, R.; Ruoslahti, E. Cancer Treatment by Targeted Drug Delivery to Tumor Vasculature in a Mouse Model. *Science* **1998**, *279*, 377–380.
(13) Chen, X.; Plasencia, C.; Hou, Y.; Neamati, N. Synthesis and Biological Evaluation of Dimeric RGD Peptide-Paclitaxel Conjugate as a Model for Integrin-Targeted Drug Delivery. *J. Med. Chem.* **2005**, *48*, 1098–1106.
(14) Anderson, M. E.; Siahaan, T. J. Mechanism of Binding and Internalization of ICAM-1-Derived Cyclic Peptides by LFA-1 on the Surface of T Cells: A Potential Method for Targeted Drug Delivery. *Pharm. Res.* **2003**, *20*, 1523–1532.
(15) Anderson, M. E.; Tejo, B. A.; Yakovleva, T.; Siahaan, T. J. Characterization of Binding Properties of ICAM-1 Peptides to LFA-1: Inhibitors of T-Cell Adhesion. *Chem. Biol. Drug Des.* **2006**, *68*, 20–28.

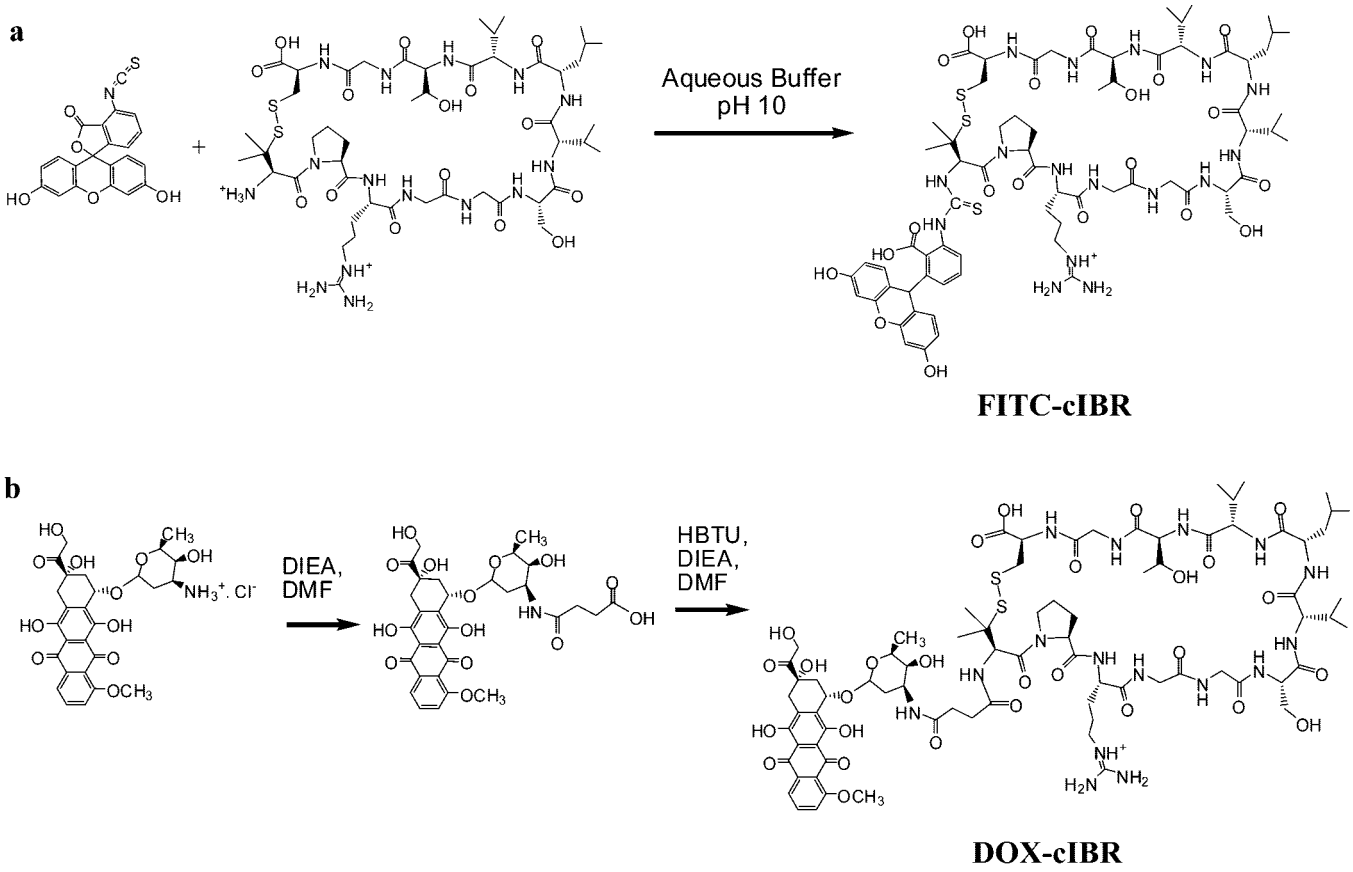

Figure 1. Structure and synthetic steps to make (a) FITC–cIBR and (b) DOX–cIBR.

ride, succinic anhydride, and diisopropylethylamine were obtained from Sigma Chemicals, Inc. (St. Louis, MO). Solvents used in peptide synthesis were of pure analytical grade. All reagents, resins, and Fmoc-protected amino acids for peptide syntheses were purchased from Peptides International, Inc. (Louisville, KY), Advanced ChemTech (Louisville, KY), and Applied Biosystems (Foster City, CA).

Peptide Synthesis. Synthesis of linear IBR peptide (Pen-PRGGSVLVTGC) was performed on a Pioneer peptide synthesizer (PerSeptive Biosystems) using the standard Fmoc solid-phase strategy with *O*-(7-azabenzotriazol-1-yl)-*N*,*N*,*N*′,*N*′-tetramethyluronium hexafluorophosphate (HATU) as the activating agent. Extended coupling cycles were employed. The resin-containing peptide was washed several times with methylene chloride and then with methanol followed by vacuum drying. A cleavage cocktail containing trifluoroacetic acid (TFA, 90%), 1,2-ethanedithiol (3%), anisole (2%), and thioanisole (5%) was used during peptide cleavage from the solid support followed by precipitation in ice-cold diethyl ether. The diethyl ether solution was allowed to stand overnight at 4 °C for maturation of the precipitate. Subsequently, the precipitate of the peptide was separated from ether-containing scavengers by centrifugation. The crude linear peptide was purified by semipreparative C18 reverse-phase HPLC. The cyclization of the linear peptide to give cIBR peptide was carried out by bubbling air for 2 h into the peptide solution (0.06 mM) containing ammonium bicarbonate (0.05 M) and ammonium hydroxide at pH 8.5. The solution was lyophilized, and crude cIBR was purified by semipreparative C18 reverse-phase HPLC. The molecular weight of cIBR peptide was determined by electrospray ionization mass spectrometry (M + 1 = 1174.5).

Conjugation of FITC with cIBR. Conjugation of FITC with cIBR was conducted according to our previously published method (Figure 1a).[16] Briefly, pure cIBR peptide (0.04 mmol) was dissolved in 5 mL of Nanopure water; 0.08 mmol of fluorescein 5-isothiocyanate (Sigma) was added to the peptide solution, and the pH was adjusted to 10 by addition of a 1.0 N NaOH solution. After being stirred for 1 h with a magnetic stirrer, the reaction mixture was neutralized by the addition of a 10% (v/v) acetic acid solution. The solution was lyophilized, and the resulting crude product of FITC-cIBR was purified by semipreparative C18 reverse-phase HPLC. The pure FITC–cIBR was analyzed by analytical C18 reverse-phase HPLC and identified by electrospray ionization mass spectrometry (M + 1 = 1563.4).

Conjugation of Doxorubicin with cIBR. In this case, the amino group in the sugar moiety of DOX was reacted with succinic anhydride in dimethylformamide (DMF) in the presence of diisopropylethylamine to give DOX-hemi-

(16) Gursoy, R. N.; Siahaan, T. J. Binding and Internalization of an Icam-1 Peptide by the Surafce Receptors of T Cells. *J. Pept. Res.* **1999**, *53*, 414–421.

succinate (M + 1 = 643) (Figure 1b). Subsequently, DOX-hemisuccinate was reacted with the N-terminus of cIBR in the presence of HBTU in DMF to give the DOX–cIBR. The progress of the reaction was monitored via C18 reverse-phase analytical HPLC. DOX–cIBR was purified using semi-preparative HPLC with a C18 column; the molecular weight of the final product was confirmed by mass spectrometry (M + 1 = 1799).

Temperature-Dependent Internalization Studies. HL-60 cells were centrifuged and resuspended in RPMI 1640 at a concentration of 1×10^6 cells/mL; 250 μL of the cell suspension was plated in two different tissue culture plates, and then, 250 μL of a solution of FITC–cIBR (100 μM), DOX–cIBR (5 μM), DOX (5 μM), and FITC-bound dextran (FITC–dextran) (200 μM, MW = 10 000; Molecular Probes, Eugene, OR) was added to the respective wells. The cells were incubated at 37 and 4 °C for 1 h while protected from light and were then transferred into 1.5 mL Eppendorf tubes and centrifuged at 1000 rpm for 2 min. The cells were washed three times with ice-cold phosphate-buffered saline (PBS) and finally suspended in 20 μL of PBS. The final cell density used for the microscopic observation was 12.5×10^6 cells/mL; 10 μL of the cell suspension was put on the slide for observation. Control cells without any compound added were treated the same way. A Nikon Eclipse 80*i* microscope equipped for epifluoroscence was used to view the cells, and the fluorescence emissions of DOX and FITC were observed using rhodamine and FITC filter sets, respectively. Untreated cells were viewed with both set of filters to check for their autofluorescence. The images were captured using an Orca ER camera (Hamamatsu, Inc., Bridgewater, NJ) controlled by Metamorph, version 6.2 (Universal Imaging Corp., West Chester, PA).

Microtubule Disruption Studies. Cells were plated as indicated above and were incubated with 50 μM nocodazole in DMSO (0.5% in PBS) for 4 h prior to addition of 250 μL of FITC–cIBR (100 μM), DOX–cIBR (5 μM), DOX (5 μM), FITC–dextran (MW = 10 000), and Oregon green (5 μM; Molecular Probes) to the wells.[17] Cells were treated with 250 μL of solution of 0.5% DMSO in PBS to check the effect of DMSO on the cells. Washing and microscopic observations were carried out in the manner described above.

Energy Depletion Studies. Cells were centrifuged and resuspended in 250 μL of a solution of either RPMI 1640 or PBS containing 50 mM 2-deoxy-D-glucose and 25 mM sodium azide and were incubated for 45 min at 37 °C in 5% CO_2.[18] Next, the cells were incubated for 1 h with 250 μL solutions of FITC–cIBR (100 μM), DOX–cIBR (5 μM), DOX (5 μM), and FITC–dextran (MW = 10 000, 200 μM). The cells were then washed three times with ice-cold PBS and finally suspended in 20 μL of PBS for microscopic observation.

Stability Studies. Exponentially growing HL-60 cells were centrifuged and resuspended in RPMI 1640 medium at a concentration of 2×10^6 cells/mL; 250 μL of the cell suspension was distributed into a 48-well tissue culture plate (BD Biosciences, San Jose, CA). Then, 250 μL of a 100 μM DOX–cIBR solution in PBS at pH 7.4 was added to each of the wells over different time periods (0, 1, 2, 14, 18, and 24 h), and the cells were incubated in a humidified atmosphere with 5% CO_2. Three samples of the cell suspension along with the compound solution at each time point were transferred to 1.5 mL Eppendorf tubes, and 500 μL of acetonitrile was added. Samples were vortexed for 2 min followed by sonication at 37 °C for 30 min. After sonication, the samples were vortexed again for 2 min and centrifuged at 14 000 rpm for 10 min. Aliquots from the supernatant (20 μL) were mixed with 20 μL of solvent (52:48 ratio of acetonitrile and water in the presence of 0.05% TFA). Each sample (20 μL) was injected into the analytical reverse-phase HPLC system with a C18 column and detected at an absorption wavelength of 480 nm. The elution was performed using a gradient program involving solvent A (95% water containing 0.1% TFA and 5% acetonitrile) and solvent B (acetonitrile). A linear gradient program from 100% A to 100% B over a period of 18 min was used with a flow rate of 1 mL/min.

Determination of the Octanol/Aqueous Buffer Distribution Ratio. One milliliter of *n*-octanol (Sigma) was added to 10 mL of PBS (pH 7.4) containing 2.0 μM DOX–cIBR or FITC–cIBR in a separatory funnel and shaken for 30 min. The two phases were allowed to equilibrate for 24 h while protected from light. The concentration of DOX–cIBR or FITC–cIBR in each phase was determined using a fluorescence spectrophotometer (RF5000U, Shimadzu Inc., Kyoto, Japan). The fluorescence intensity of DOX–cIBR or FITC–cIBR in aqueous buffer solutions was measured at different concentrations, and a calibration curve was generated using Microcal Origin, version 6.0.

Internalization Studies with HUVEC. HUVEC were grown to confluency in a 75 cm^2 tissue culture flask. Confluent cells were trypsinized and resuspended in 20 mL of fresh DMEM. Sterile coverslips were placed in six-well plates, and 2 mL of the cell suspension was added to each of the wells. Cells were allowed to grow for 24 h. Before the experiment, the coverslips were checked for cell attachment, and each coverslip was washed three times to remove the unattached cells. Coverslips with a relatively similar cell attachment were used for the experiment; 500 μL of fresh DMEM was added to each well followed by 500 μL of FITC–cIBR (100 μM), DOX–cIBR (5 μM), FITC–dextran (MW = 10 000, 200 μM). Cells were incubated with the compounds for 1 h, washed three times with ice-cold PBS, and observed under a microscope.

(17) Gong, Y.; Duvvuri, M.; Duncan, M. B.; Liu, J.; Krise, J. P. Niemann-Pick C1 Protein Facilitates the Efflux of the Anticancer Drug Daunorubicin from Cells According to a Novel Vesicle-Mediated Pathway. *J. Pharmacol. Exp. Ther.* **2006**, *316*, 242–247.

(18) Potocky, T. B.; Menon, A. K.; Gellman, S. H. Cytoplasmic and Nuclear Delivery of a Tat-Derived Peptide and a β-Peptide after Endocytic Uptake into Hela Cells. *J. Biol. Chem.* **2003**, *278*, 50188–50194.

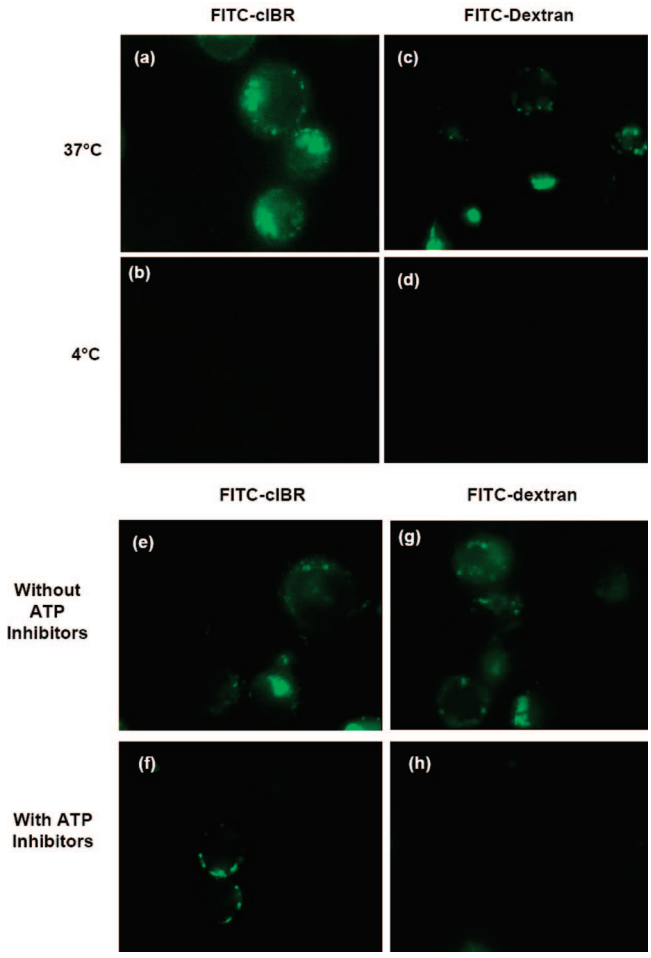

Figure 2. Comparison of the intracellular localization of FITC–cIBR and FITC–dextran in HL-60 cells observed using a fluorescence microscope. Temperature-dependent endocytosis process of FITC–cIBR incubated at (a) 37 and (b) 4 °C compared to that of FITC–dextran incubated at (c) 37 and (d) 4 °C. Comparison of the endocytosis process of FITC–cIBR in the (e) absence and (f) presence of ATP inhibitors compared to that of FITC–dextran in the (g) absence and (h) presence of ATP inhibitors.

Results

Evaluation of the Mechanism of the Cellular Entry of FITC–cIBR. The mechanism of endocytosis of FITC–cIBR was compared to that of FITC–dextran using HL-60 cells under different conditions (Figure 2). FITC–dextran, which has been used as a marker for fluid-phase endocytosis, was used as a positive control.[19–21] To evaluate the effect of cellular metabolism on the internalization of FITC–cIBR, it was incubated at two different temperatures, 37 °C (Figure 2a) and 4 °C (Figure 2b). At 37 °C, punctate fluorescence stains of FITC–cIBR were found in the endocytic compartments of HL-60 (Figure 2a) similar to those of FITC–dextran (Figure 2c). In contrast, there were no punctate stains observed when the cells were incubated with FITC–cIBR (Figure 2b) and FITC–dextran (Figure 2d) at 4 °C. This indicates the possibility of receptor-mediated uptake of FITC-cIBR. For incubation at 4 °C, there was a lack of fluorescence on the cell surface of FITC–cIBR-treated cells; therefore, it is difficult to distinguish between receptor-mediated endocytosis and fluid-phase endocytosis.

To further evaluate whether there is a difference between the mechanisms of endocytosis of FITC–cIBR (Figure 2e,f) and FITC–dextran (Figure 2g,h), the cells were incubated with ATP inhibitors (sodium azide and 2-deoxy-D-glucose) prior to incubation with FITC–cIBR and FITC–dextran. The presence of ATP inhibitors clearly inhibits the endocytosis of both FITC–cIBR (Figure 2f) and FITC–dextran (Figure 2h). However, the cells treated with FITC–cIBR in the presence of inhibitors exhibited punctate staining around the cell membranes (Figure 2f), and cells treated with FITC–dextran did not (Figure 2h). The FITC–cIBR-treated cells showed clusters of dots that also suggested the formation of receptor clusters prior to internalization. It is clear that there is a difference between the internalization of FITC–cIBR and FITC–dextran; it is also implied that FITC–cIBR is internalized by a receptor-mediated process and not via fluid-phase endocytosis.

Next, the effect of a microtubule-disrupting agent, nocodazole, on the cellular uptake of FITC–cIBR was compared to its effect on the uptake of FITC–dextran and Oregon green (Figure 3). Nocodazole blocked the cellular entry of FITC–cIBR (Figure 3a,b) as well as FITC–dextran (Figure 3c,d); however, it did not block the entry of Oregon green (Figure 3e,f). Nocodazole blocks the movement of early endosomes along the endocytic pathway or blocks the cellular entry of a molecule taken up by the endocytosis process. This suggests that the intact microtubule network is necessary for the receptor-mediated uptake of FITC–cIBR as well as the fluid-phase uptake of FITC–dextran.

Comparison of the Intracellular Distribution of DOX and DOX–cIBR. The possibility of utilizing cIBR peptide to target DOX to HL-60 cells was evaluated using DOX–cIBR. The intracellular distributions of DOX–cIBR were compared to those of DOX alone by observing the fluorescence of DOX at an emission λ of 540 nm after excitation at a λ of 480 nm. Because DOX is toxic, the viability of cells at the concentration used for uptake studies was evaluated using Trypan blue staining to ensure that DOX did not induce cell death during the study. Neither DOX nor DOX–cIBR killed HL-60 cells under the conditions used for the uptake studies. At 37 °C, DOX–cIBR was found primarily in the cytoplasm, and there was no distribution of the molecules at the endosomes or nucleus (Figure 4a). Although there was a decrease in the intensity of DOX–cIBR

(19) Stenbeck, G.; Horton, M. A. Endocytic Trafficking in Actively Resorbing Osteoclasts. *J. Cell Sci.* **2004**, *117*, 827–836.
(20) Thilo, L.; Stroud, E.; Haylett, T. Maturation of Early Endosomes and Vesicular Traffic to Lysosomes in Relation to Membrane Recycling. *J. Cell Sci.* **1995**, *108* (Part 4), 1791–1803.
(21) Baravalle, G.; Schober, D.; Huber, M.; Bayer, N.; Murphy, R. F.; Fuchs, R. Transferrin Recycling and Dextran Transport to Lysosomes Is Differentially Affected by Bafilomycin, Nocodazole, and Low Temperature. *Cell Tissue Res.* **2005**, *320*, 99–113.

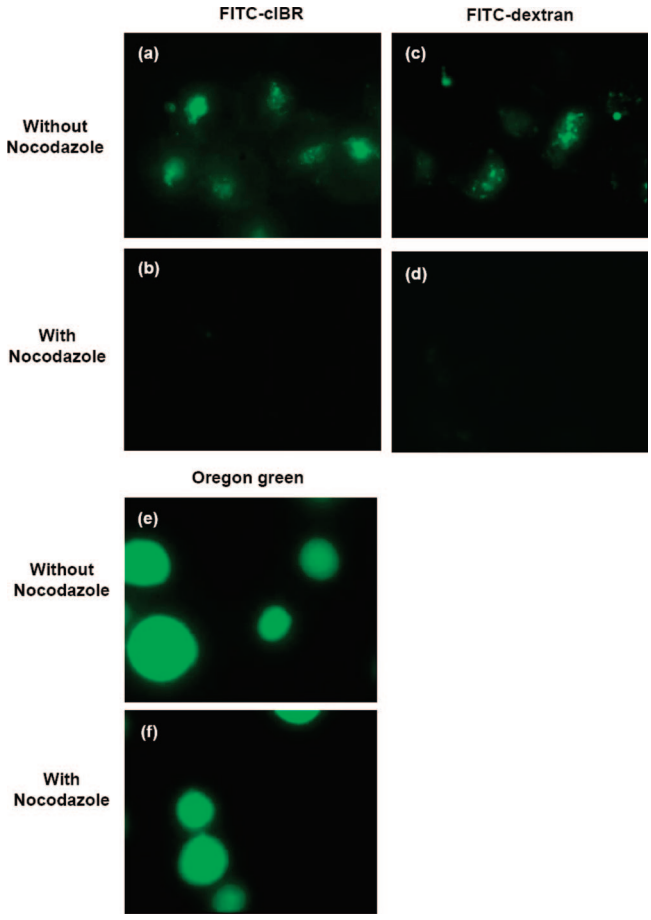

Figure 3. Effect of nocodazole on the endocytosis of FITC–cIBR, FITC–dextran, and Oregon green. Effect of the (a) absence and (b) presence of nocodazole on the endocytosis of FITC–cIBR compared to the endocytosis of FITC–dextran in the (c) absence and (d) presence of nocodazole. As a negative control, Oregon green uptake was compared in the (e) absence and (f) presence of nocodazole.

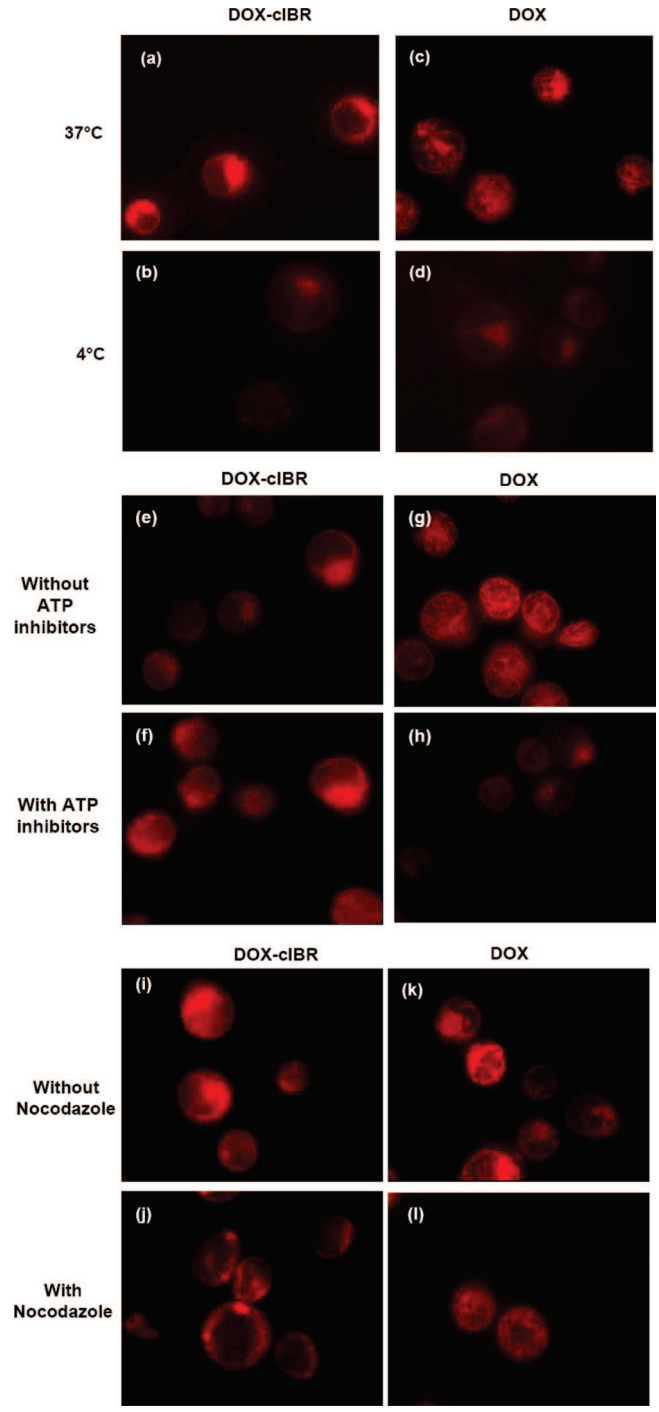

Figure 4. Comparison of the intracellular localization of DOX–cIBR and DOX in HL-60 cells incubated under different conditions. Uptake of DOX–cIBR when incubated at (a) 37 and (b) 4 °C compared to the uptake of DOX when incubated at (c) 37 and (d) 4 °C. Uptake of DOX–cIBR in the (e) absence and (f) presence of ATP inhibitors compared to the uptake of DOX in the (g) absence and (h) presence of ATP inhibitors. Comparison of the uptake of DOX–cIBR in the (i) absence and (j) presence of nocodazole to the uptake of DOX in the (k) absence and (l) presence of nocodazole.

in the cytoplasm of HL-60 cells when cells were incubated at 4 °C, there was no inhibition of uptake of DOX–cIBR (Figure 4b). This suggests that conjugation of DOX to cIBR alters the receptor-mediated endocytic uptake process of DOX–cIBR compared to that of FITC–cIBR (see above). DOX incubated at 37 °C exhibited a strong distribution at the nucleus with a weaker distribution in the cytoplasm (Figure 4c). Migration of DOX into the nucleus has been shown to be time- and concentration-dependent. Lowering the incubation temperature from 37 to 4 °C inhibited the uptake of DOX to some degree, and its distribution was shown in the nucleus as well as the cytoplasm (Figure 4d).

The effect of the energy-dependent process of DOX–cIBR uptake was evaluated by incubating the HL-60 cells with sodium azide and 2-deoxy-D-glucose for 1 h prior to incubation in DOX–cIBR. The results showed that there was no difference in the cell cytoplasmic fluorescence from DOX–cIBR on untreated (Figure 4e) or treated (Figure 4f) cells. This suggests that DOX–cIBR could still enter the cell cytosol in the absence of ATP. Similarly, DOX alone was also not affected by the inhibition of energy-dependent

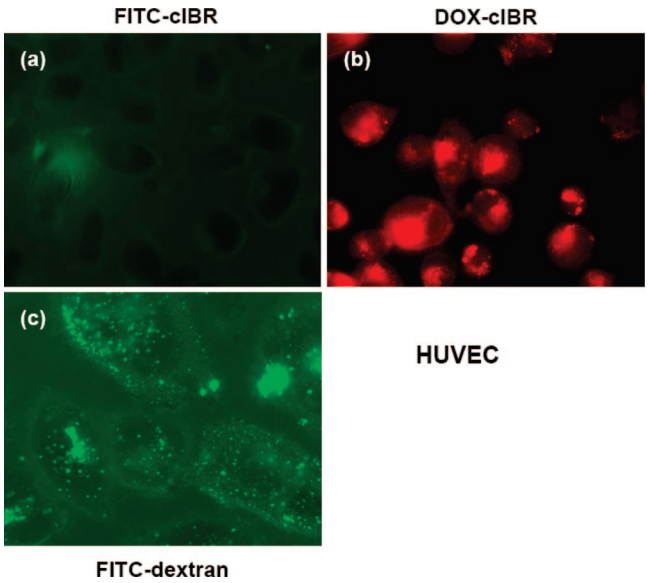

Figure 5. Comparison of internalization of (a) FITC–cIBR, (b) DOX–cIBR, and (c) FITC–dextran in HUVEC, which are deficient in LFA-1 receptors.

processes (Figure 4g,h). As shown previously, entry of FITC–dextran into cells was blocked by the inhibitors. These results indicate that the major route of entry of DOX–cIBR into HL-60 cells is possibly via passive diffusion rather than the receptor-mediated endocytic process.

HL-60 cells were also incubated with nocodazole to evaluate the effect of microtubule disruption on the entry of DOX–cIBR compared to that of DOX, Oregon green, and FITC–dextran. The fluorescence intensity of DOX–cIBR in the cell cytoplasm was not distinguishable in the absence (Figure 4i) and presence (Figure 4j) of nocodazole, suggesting that DOX–cIBR internalization does not involve microtubule formation. Similarly, the fluorescence intensity in the cells appeared to be slightly lower in the presence (Figure 4l) of nocodazole than in its absence (Figure 4k). This difference suggests that the mechanism of entry of DOX might not be solely via passive diffusion. In addition, once DOX is inside the cell, disruption of cellular systems by nocodazole can influence the distribution of DOX inside the cell. Taken together, these results suggest that the major route of cellular uptake of DOX–cIBR and DOX was not via a receptor-mediated endocytic process but via passive diffusion.

Comparison of Uptake of FITC–cIBR and DOX–cIBR by HUVEC. To confirm that FITC–cIBR was internalized via receptor-mediated endocytosis (i.e., LFA-1) and that DOX–cIBR entered the cells via passive diffusion, their uptakes were studied in HUVEC monolayers. In contrast to HL-60 cells, HUVEC do not have the LFA-1 receptor that recognizes the cIBR peptide. The results showed that FITC–cIBR was not found in the endosomic compartments as well as in the cytoplasmic domain of HUVEC (Figure 5a), indicating the necessity of the LFA-1 receptor for the entry of FITC–cIBR. In contrast, DOX–cIBR was found in

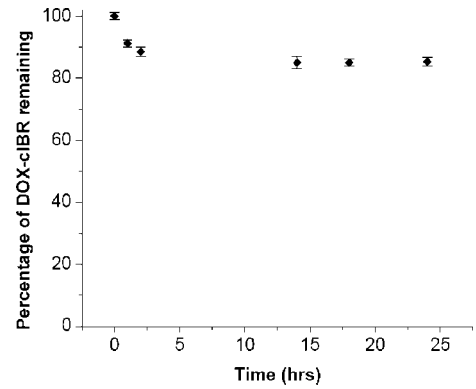

Figure 6. Time-dependent stability of DOX–cIBR in medium containing HL-60 cells determined by C18 reverse-phase HPLC. The percent of DOX–cIBR remaining was determined by integrating the area under the curve for DOX–cIBR at a detection wavelength of 480 nm. Each point represents an average of three experiments.

the cytoplasm of HUVEC (Figure 5b), suggesting that this molecule entered the cell via passive diffusion as in HL-60 cells. As a positive control, FITC–dextran was found in the endosomic compartments of HUVEC (Figure 5c) as it entered the cells via fluid-phase endocytosis. These results suggest that the entry of FITC–cIBR is mediated by receptors, especially LFA-1, which is found in HL-60 cells but not in HUVEC and that DOX–cIBR can passively diffuse in both HUVEC and HL-60 cells.

Physicochemical Properties of DOX–cIBR and FITC–cIBR. The stability of DOX–cIBR was evaluated in the presence of HL-60 cells using the same conditions that were used in the experiments for the endocytic uptake process. This was done to make sure that the presence of fluorescence in the cytoplasm of HL-60 cell was due to the intact DOX–cIBR and not to its degradation products (e.g., free DOX). DOX–cIBR was incubated for 24 h with HL-60 cells, and the cells were isolated and lysed with acetonitrile at different time points. After removal of the cell debris by centrifugation, the acetonitrile supernatant solution was injected into an analytical HPLC system with a C18 column. The disappearance of DOX–cIBR and the appearance of new peaks due to the degradation of DOX–cIBR were monitored at 480 nm to avoid interference from the proteins derived from the medium and cells. The area under the curve from the DOX–cIBR peak was integrated as a function of time (Figure 6). The results showed that 11.5% degradation of DOX–cIBR was observed in the first 2 h of incubation; prolonged incubation for up to 24 h produced only 15% degradation. The results suggest that that the majority of DOX–cIBR is intact during the 24 h incubation in endocytic studies and that the fluorescence stains found inside the cell are due to DOX–cIBR.

To compare the difference in lipophilicity between FITC–cIBR and DOX–cIBR conjugates, the octanol/water distribution ratios for both compounds were determined to predict the possibility of the conjugates entering the cells via passive

Table 1. Experimentally Determined Distribution Ratios for DOX–cIBR and FITC–cIBR at pH 7.4[a]

	distribution ratio (*D*)	Log D
DOX–cIBR	14.1	1.15
FITC–cIBR	3.8	0.58
DOX	1.23 (2.4[b])	0.08

[a] Values are means of three determinations. [b] Value from the literature.

diffusion (Table 1). Normally, small molecules with high lipophilicity with a Log D between 1 and 3 can readily partition to cell membranes and enter the cells via passive diffusion. The results show that FITC–cIBR (Log D = 0.58) is more hydrophilic than DOX–cIBR (Log D = 1.14) but FITC–cIBR is less hydrophilic than DOX (Log D = 0.08). The high hydrophobicity of DOX–cIBR explains its effective partitioning into the cell membranes and passive permeation into the cell. Although FITC–cIBR is more hydrophobic than DOX, it does not partition into the membrane as effectively as the smaller DOX; this may be due to the large size of FITC–cIBR compared to DOX and to its higher hydrogen bonding potential with water.

Discussion

We have shown that FITC–cIBR is internalized by HL-60 via receptor-mediated endocytosis. The endocytosis could be due to the presence of LFA-1 on the HL-60 cells and properties of binding of FITC–cIBR to LFA-1; LFA-1 receptors have been shown to be internalized and recycled by leukocytes.[22] In addition, the LFA-1-deficient HUVEC did not internalize FITC–cIBR. FITC–cIBR had been shown to bind to isolated LFA-1 and LFA-1 on the surface of T cells; this binding process could be inhibited by unlabeled cIBR peptide as well as antibodies to the I domain of LFA-1.[14] FITC–cIBR could colocalize with anti-β_2-antibodies on the surface of T cells, suggesting that this peptide binds β_2 integrins such as LFA-1.[14] MOLT-3 and SKW T cells could take up FITC–cIBR; however, due to the size of T cells, it was difficult to study the intracellular trafficking of FITC–cIBR in T cells compared to that in HL-60 cells.[14,16] The binding site of FITC–cIBR is at the L site, and a possible second binding site is in the MIDAS region of the LFA-1 I domain.[15] Due to the leukocyte selectivity of FITC–cIBR, the possibility of using cIBR peptide to target the anticancer drug DOX to leukemic cells (i.e., HL-60 cells, MOLT-3 T cells) was investigated. DOX has been shown to be a good model drug for conjugation of carrier molecules (i.e., peptides, proteins, carbohydrates, and polymers) for targeted drug delivery because its entry into the cell can be monitored by fluorescence microscopy. Thus, the endocytosis mechanism of DOX–cIBR was compared to that of FITC–cIBR with the expectation that both molecules would be internalized via a receptor-mediated endocytosis process.

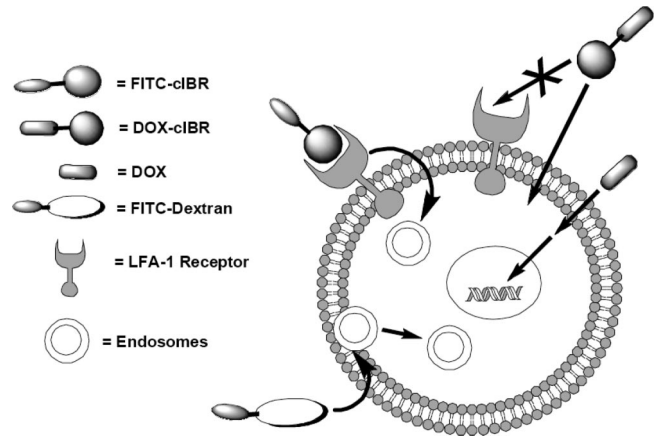

Figure 7. Schematic representation of the cellular entry mechanism of FITC–cIBR, FITC–dextran, DOX–cIBR, and DOX in HL-60 cells. FITC–cIBR enters the cells via a receptor-mediated process via the endosomes, while FITC–dextran enters the endosomes via fluid-phase endocytosis. On the other hand, DOX–cIBR passively permeates through the cell membranes and resides in the cytoplasm, and DOX enters the cell via passive diffusion and finally resides in the nucleus.

It was interesting to find that DOX–cIBR passively diffused through the cell membrane of HL-60 cells, which was contrary to the case for FITC–cIBR. The change in the internalization behavior of these two conjugates can be due to many different factors. First, the high hydrophobicity of DOX–cIBR compared to that of FITC–cIBR (Table 1) may alter its mechanism of entry into the cells. It is possible that a small fraction of DOX–cIBR was internalized via a receptor-mediated process; however, due to the high fraction that partition into the cell membranes, the receptor-mediated process was overwhelmed by the passive diffusion mechanism (Figure 7). Second, the conjugation of DOX to cIBR may dramatically change the conformation of cIBR peptide compared to the conjugation of FITC to cIBR. The dramatic change in the conformation of cIBR prevents the recognition of the cIBR fragment of DOX–cIBR by the receptor (i.e., LFA-1) on the cell surface. Our previous studies have shown that the recognition site of cIBR peptide is at the Pro-Arg-Gly-Gly (PRGG) sequence, which resides at the N-terminus.[23] The PRGG sequence is in a stable β-turn structure as determined by NMR;[24] conjugation of the N-terminus with another drug, methotrexate, did not change the β-turn conformation of this recognition site. Finally, it is also

(22) Fabbri, M.; Di Meglio, S.; Gagliani, M. C.; Consonni, E.; Molteni, R.; Bender, J. R.; Tacchetti, C.; Pardi, R. Dynamic Partitioning into Lipid Rafts Controls the Endo-Exocytic Cycle of the αL/β2 Integrin, LFA-1, During Leukocyte Chemotaxis. *Mol. Biol. Cell* **2005**, *16*, 5793–5803.

(23) Anderson, M. E.; Yakovleva, T.; Hu, Y.; Siahaan, T. J. Inhibition of ICAM-1/LFA-1-Mediated Heterotypic T-Cell Adhesion to Epithelial Cells: Design of Icam-1 Cyclic Peptides. *Bioorg. Med. Chem. Lett.* **2004**, *14*, 1399–1402.

(24) Gursoy, R. N.; Jois, D. S.; Siahaan, T. J. Structural Recognition of an ICAM-1 Peptide by Its Receptor on the Surface of T Cells: Conformational Studies of Cyclo (1,12)-Pen-Pro-Arg-Gly-Gly-Ser-Val-Leu-Val-Thr-Gly-Cys-OH. *J. Pept. Res.* **1999**, *53*, 422–431.

possible that the DOX fragment imposes steric hindrance on the recognition site of cIBR peptide as compared to that of the FITC fragment in FITC–cIBR. Because both DOX and FITC are conjugated to the N-terminus, there is a high probability that conjugation of a moiety to the N-terminus may interfere with the recognition of cIBR. Therefore, further structural studies will be carried out to elucidate the effect of conjugation of DOX to the cIBR structure.

Normally, the passive diffusion mechanism is used by small hydrophobic drugs such as doxorubicin with molecular masses of 500 Da following Lipinski's rules;[25] these molecules readily partition into cell membranes to cross the lipid bilayers. In contrast, large hydrophilic peptides with a high hydrogen bonding potential are not readily partitioned into the cell membranes because it is energetically unfavorable to expel hydrogen-bonded water molecules.[25] However, DOX–cIBR has an octanol/water distribution ratio that is very high compared to those of FITC–cIBR and DOX (Table 1). The high distribution ratio of DOX–cIBR could explain the strong propensity of DOX–cIBR to partition to cell membranes for passive diffusion. It is possible that conjugating DOX to cIBR peptide causes an altered conformation of the conjugate to produce low hydrogen bonding potential to water molecules. On the basis of the magnitude of the distribution ratio alone, FITC–cIBR should passively diffuse more readily than DOX alone. Instead, FITC–cIBR is internalized by a receptor-mediated process, and DOX enters the cell mainly via passive diffusion. We propose that there is a balance between passive diffusion and the receptor-mediated mechanism, depending on the moiety or drug molecule that is attached to the cIBR peptide (Figure 7). If this is the case, the choice of the drug molecule that can be conjugated to cIBR to maintain the receptor-mediated internalization properties may be limited to drugs that do not dramatically change the octanol/water distribution ratio. In other words, the distribution ratio of the conjugate should be at least similar to or lower than that of FITC–cIBR for receptor-mediated entry into the cells.

Others have conjugated DOX to peptides, proteins, oligonucleotides, and other types of carriers. The conjugate of DOX with the cell-penetrating peptide exhibited a cytoplasmic distribution of the conjugate similar to that in DOX–cIBR. Unfortunately, it is not clear whether the DOX conjugate with cell-penetrating peptides enters the cell via passive diffusion or via receptor-mediated endocytosis.[26] In another study, DOX was also conjugated to a cyclic pentapeptide (CNGRC) to give the DOX–CNGRC conjugate for targeting CD13 on the surface of the SK-UT-1 cell line.[27] Similar to our DOX–cIBR, the DOX–CNGRC conjugate was found in the cell cytoplasm. It has been suggested that the uptake of DOX–CNGRC is not via receptor-mediated but via passive diffusion because DOX–CNGRC has a high octanol/water distribution coefficient (5.3).[27] This distribution coefficient is between those of DOX–cIBR (14.1) and FITC–cIBR (3.8). It was surprising to find that the DOX–transferrin conjugate is distributed in the cytoplasm, and its entry into the cells could not be blocked by transferrin or a lower temperature.[9,28] These results suggest that this conjugate entry was not mediated by the transferrin receptor. Because transferrin is a large molecule, it is difficult to envision that this conjugate could penetrate the cell membrane through passive diffusion. Another possible explanation is that conjugation of the molecule to DOX may alter the conjugate physical properties and induce the formation of a molecular association that promotes partitioning into cell membrane and permeation into the cytoplasm. Regen et al.[29–31] have proposed possible mechanisms (i.e., umbrella mechanism) of membrane partitioning of a conjugate between a sugar molecule and an oligonucleotide or a peptide that led to cell membrane permeation. Because DOX contains an amino sugar moiety, DOX–peptide conjugates may follow the umbrella mechanism to enter the cells via the passive route. Thus, DOX rather than the peptide becomes the important molecule for membrane partitioning; however, further studies need to be done to elucidate this possible mechanism.

The uptake of DOX–cIBR and DOX was affected by temperature; lower fluorescence intensities of these molecules were found in the cytoplasm at 4 °C than at 37 °C. It has been suggested that slower diffusion of DOX at 4 °C than at 37 °C is due to the increase in the level of self-association of DOX at 4 °C via the formation of π-interactions.[32] The effect of temperature on the uptake of DOX–cIBR could also be caused by the formation of self-association of the conjugate at 4 °C. Alternatively, DOX–cIBR could enter the cell via a combination of passive and active transport at 37 °C but only via passive permeation at 4 °C. A similar hypothesis has been suggested for the internalization of the DOX–transferrin conjugate.[9] Due to the high octanol/water

(25) Lipinski, C. A.; Lombardo, F.; Dominy, B. W.; Feeney, P. J. Experimental and Computational Approaches to Estimate Solubility and Permeability in Drug Discovery and Development Se. *Adv. Drug Delivery Rev.* **2001**, *46*, 3–26.

(26) Liang, J. F.; Yang, V. C. Synthesis of Doxorubicin-Peptide Conjugate with Multidrug Resistant Tumor Cell Killing Activity. *Bioorg. Med. Chem. Lett.* **2005**, *15*, 5071–5075.

(27) van Hensbergen, Y.; Broxterman, H. J.; Elderkamp, Y. W.; Lankelma, J.; Beers, J. C.; Heijn, M.; Boven, E.; Hoekman, K.; Pinedo, H. M. A Doxorubicin-CNGRC-Peptide Conjugate with Prodrug Properties. *Biochem. Pharmacol.* **2002**, *63*, 897–908.

(28) Lai, B. T.; Gao, J. P.; Lanks, K. W. Mechanism of Action and Spectrum of Cell Lines Sensitive to a Doxorubicin-Transferrin Conjugate. *Cancer Chemother. Pharmacol.* **1998**, *41*, 155–160.

(29) Janout, V.; Jing, B.; Regen, S. L. Molecular Umbrella-Assisted Transport of an Oligonucleotide across Cholesterol-Rich Phospholipid Bilayers. *J. Am. Chem. Soc.* **2005**, *127*, 15862–15870.

(30) Jing, B.; Janout, V.; Herold, B. C.; Klotman, M. E.; Heald, T.; Regen, S. L. Persulfated Molecular Umbrellas as Anti-HIV and Anti-HSV Agents. *J. Am. Chem. Soc.* **2004**, *126*, 15930–15931.

(31) Jing, B.; Janout, V.; Regen, S. L. Fully Detachable Molecular Umbrellas as Peptide Delivery Agents. *Bioconjugate Chem.* **2003**, *14*, 1191–1196.

(32) Dalmark, M.; Storm, H. H. A Fickian Diffusion Transport Process with Features of Transport Catalysis. Doxorubicin Transport in Human Red Blood Cells. *J. Gen. Physiol.* **1981**, *78*, 349–364.

partition coefficient of DOX–cIBR, the passive diffusion pathway overwhelms the receptor-mediated transport of DOX–cIBR at 37 °C (Figure 7). As seen for FITC–cIBR, cIBR peptide did not show any cell surface staining when incubated at 4 °C, suggesting that the binding of cIBR peptide to LFA-1 was low at low temperatures. An alternative explanation is that the cells have a higher population of inactive LFA-1 at 4 °C. Similarly, DOX–cIBR did not exhibit any cell surface staining at 4 °C, suggesting that it did not bind to the cell surface receptors. Unfortunately, unlike the case with FITC–cIBR, it is difficult to differentiate between the cytoplasmic and cell surface staining when HL-60 cells are treated with DOX–cIBR in the presence of ATP inhibitors at 37 °C.

In conclusion, we have shown that FITC–cIBR peptide can be internalized via a receptor-mediated pathway, suggesting that cIBR peptide is internalized by the LFA-1 receptor on HL-60 cells. However, the use of hydrophobic drugs such as DOX in the DOX–cIBR conjugate may change receptor-mediated transport to passive diffusion transport. This study has shown the importance of the physicochemical properties of the drug–peptide conjugate when considering the use of the peptide for cell-specific targeted drug delivery. We postulate that, to maintain the high propensity of using the receptor-mediated endocytic pathway, a hydrophilic drug should be used to conjugate to the cIBR peptide and that the octanol/water distribution ratio of the conjugate should be at least the same as or lower than the distribution ratio of FITC–cIBR. The effect of different drug properties on the receptor-mediated endocytosis of drug–cIBR conjugates is currently being investigated. We hope to find an appropriate anticancer drug that can target LFA-1-expressing leukemic cells.

Acknowledgment. This work is supported by the National Institutes of Health (Grant R01-AI-063002). We thank the American Heart Association, Heartland Affiliate, for the postdoctoral fellowship to N.K. We also thank Nancy Harmony for proofreading the manuscript.

MP0700458